MAGMA (2005) 18: 225–230
DOI 10.1007/s10334-005-0122-8

RESEARCH ARTICLE

C.H. Ziener
W.R. Bauer
P.M. Jakob

Frequency distribution and signal formation around a vessel

Received: 17 May 2005
Revised: 19 July 2005
Accepted: 19 July 2005
Published online: 20 September 2005

C. H. Ziener (✉) · P. M. Jakob
Bayerische Julius-Maximilians-Universität Würzburg,
Lehrstuhl für Experimentelle Physik 5, Am Hubland, 97074 Würzburg, Germany
Tel.: +49-931-8884957
Fax: +49-931-8885861
E-mail: ziener@physik.uni-wuerzburg.de

W. R. Bauer
Bayerische Julius-Maximilians-Universität Würzburg,
Medizinische Universitätsklinik,
Josef-schneider-Strasse 2, 97080 Würzburg, Germany

Abstract We describe the NMR signal formation properties of a single vessel. Instead of assuming the frequency distribution to be a simple Lorentzian or Gaussian one, we take into account that the frequency distribution around the vessel is a complex function. Considering the static dephasing regime we find a relationship between signal formation and frequency distribution. Analytical expressions for the frequency distribution in a voxel and the magnetization decay are obtained. In the case of small volume fractions of blood and week magnetic fields the results can be used for describing signal formation processes in a vascular network. A relationship between the frequency distribution and the properties of the vascular network is derived. The magnetization decay in different time regimes is discussed. The result is relevant for describing signal formation processes around a vessel for arbitrary pulse sequences.

Keywords Susceptibility effects · Spin dephasing · Frequency distribution

Introduction

Susceptibility effects and their influence on signal formation are highly interesting in magnetic resonance imaging (MRI). For example, the paramagnetic property of deoxygenated hemoglobin induces a susceptibility difference between blood vessels and surrounding tissue. The generated internal magnetic field and the resulting frequency distribution determine the MR properties of the tissue. Focusing on the gradient echo relaxation time, Kennan et al. [1] compared a Gaussian and Cauchy distribution of local frequencies and noted that the precise field dependence of gradient echo relaxation depends on the choice of $p(\omega)$ and is in general not known. The exact description of this frequency distribution is the aim of this work.

The signal formation in the static dephasing regime was first developed by Yablonskiy and Haacke [2] in 1994. The theory of transverse relaxation has been significantly developed since that time, mainly by Yablonskiy [2–4], Bauer [5–7], Kiselev [8–10], and Jensen and Chandra [11, 12]. Following the approach of Yablonskiy and Haacke we consider the static dephasing regime to find a relationship between signal formation and frequency distribution.

In general, an MRI experiment is determined completely by the used pulse sequence and the scanned tissue. The tissue is characterized by the distribution of dephasing frequencies $p(\omega)$. The signal obtained from a voxel is the sum over all spins emitting transverse magnetization $M_x(\omega) + i M_y(\omega)$ multiplied by their probability distribution $p(\omega)$ and can be extended to the following expression [13–15]:

$$M(t) = \int_{-\infty}^{+\infty} p(\omega) \left[M_x(\omega) + i M_y(\omega) \right] \mathrm{e}^{i\omega t} \, \mathrm{d}\omega \,. \tag{1}$$

This paper focuses on the exact form of the distribution of the off-resonance frequencies $p(\omega)$. In the special case of a FLASH sequence [16], the response profile $M_x(\omega) + i M_y(\omega)$ is a constant, and therefore the signal $M(t)$ is the Fourier transform of the frequency distribution. Now the question arises of how to describe experiments with more sophisticated response profiles. Therefore, it is necessary to know the exact form of the distribution of dephasing frequencies $p(\omega)$, which is deduced and analyzed in this study.

Methods

The BOLD effect arises from the paramagnetic property of deoxyhemoglobin [17]. A single vessel containing blood that is surrounded by water is a simple example of susceptibility effects caused by the properties of blood. We assume the vessel to be a cylindrical capillary with radius R_C embedded in a voxel. For arriving at simple analytical expressions we consider the voxel as a surrounding concentric cylinder with radius R.

The BOLD-related transverse relaxation of spins is induced by the inhomogeneous magnetic field around the capillary. Dephasing mechanisms caused by the imaging gradients as considered by Mattiello et al. [18] are neglected. The inhomogeneous field around a capillary in cylindrical coordinates (r, ϕ) is given by

$$B(\mathbf{r}) = \frac{\Delta\chi}{2} B_0 \, \sin^2\theta \, R_C^2 \, \frac{\cos 2\phi}{r^2} \,, \tag{2}$$

where $\Delta\chi$ is the difference of the susceptibility between the capillary and the surrounding tissue [19] and θ is the tilt angle to the external field. Introducing the characteristic equatorial frequency shift

$$\begin{aligned} \delta\omega_\theta &= \gamma \, B(r = R_C, \phi = 0) \\ &= \gamma \, \frac{\Delta\chi}{2} B_0 \, \sin^2\theta \,, \end{aligned} \tag{3}$$

where γ is the gyromagnetic ratio, we have

$$\omega(\mathbf{r}) = \delta\omega_\theta \, R_C^2 \, \frac{\cos 2\phi}{r^2} \,. \tag{4}$$

The field inside the capillary $B_{\mathrm{int}} = \Delta\chi \, B_0 (3\cos^2\theta - 1)/6$ is independent of the distance to the axis of the cylinder [19] and leads to an internal local frequency $\omega_{\mathrm{int}} = 2\delta\omega_{\pi/2}/3 - \delta\omega_\theta$. Based on the picture of spins diffusing around the capillary, two frequency scales are present, each characterizing one underlying relaxation mechanism: the dynamic frequency scale and the magnetic frequency scale. The dynamic frequency scale is characterized by the inverse of the correlation time $1/\tau = D/R_C^2$, while the magnetic frequency scale is described by the equatorial frequency shift $\delta\omega_\theta$. We will focus our attention on the case where the $\delta\omega_\theta$ dominates, i.e., we assume static dephasing conditions. The NMR signal decay due to the magnetic moment dephasing resulting from the local differences in the nuclear frequencies occurs faster than the diffusion phenomena manage to average out the phases of different nuclei [2]. The NMR signal in the static dephasing regime $M(t)$ may be presented as

$$M(t) = \frac{1}{V} \int_V \mathrm{d}^3\mathbf{r} \; \rho(\mathbf{r}) \, \mathrm{e}^{\mathrm{i}\,\omega(\mathbf{r})\,t} \,, \tag{5}$$

where V is the relaxation volume, i.e., the coaxial cylinder with radii R_C and R as described above. The local resonance frequency at medium point $\mathbf{r}$ is $\omega(\mathbf{r})$, and $\rho(\mathbf{r})$ is the spin density [2, 20–22]. Introducing the Dirac distribution leads to the following expression for the signal:

$$\begin{aligned} M(t) \; &= \; \frac{1}{V} \int_V \mathrm{d}^3\mathbf{r} \; \rho(\mathbf{r}) \int_{-\infty}^{+\infty} \mathrm{d}\omega \; \delta[\omega - \omega(\mathbf{r})] \mathrm{e}^{\mathrm{i}\,\omega t} \\ &= \; \rho_0 \int_{-\infty}^{+\infty} \mathrm{d}\omega \; p(\omega) \, \mathrm{e}^{\mathrm{i}\,\omega t} \,. \end{aligned} \tag{6}$$

Adapting methods of statistical physics [20, 23], we are able to define a distribution function of the Larmor frequency in the following way:

$$p(\omega) = \frac{1}{\rho_0 V} \int_V \mathrm{d}^3\mathbf{r} \; \rho(\mathbf{r}) \, \delta[\omega - \omega(\mathbf{r})] \,, \tag{7}$$

which has the properties of a probability density

$$\int_{-\infty}^{+\infty} \mathrm{d}\omega \, p(\omega) = 1 \quad \text{and} \quad p(\omega) \geq 0 \,. \tag{8}$$

The expression for the distribution function of the Larmor frequency in Eq. 7 coincides with the definition of the density of states in quantum mechanics. A more intuitive way to introduce this distribution function of the Larmor frequency is to describe the presence of magnetic material in terms of a histogram [24]. Therefore, the relaxation volume is divided into small subvoxels and the local resonance frequency ω is determined for each small subvoxel. The histogram is the number N of subvoxels with a given local resonance frequency ω plotted over the local resonance frequency ω. For the specific case of a spherical object, the distribution function of the Larmor frequency for different voxel forms has been analyzed by Seppenwoolde et al. [25].

Results

To obtain an analytical expression for the distribution function of the Larmor frequency, we perform the integration in Eq. 7 using the local frequency from Eq. 4. The integration volume V is the relaxation volume according to the capillary model described above. Further we assume the spin density $\rho(\mathbf{r}) = \rho_0 = M(0)$ as a constant within the relaxation volume V. The calculation is straightforward and we obtain the expression

$$p(\omega) = \begin{cases} \frac{\eta}{1-\eta} \, \frac{\delta\omega_\theta}{\pi\omega^2} \sqrt{1 - \left(\frac{\omega}{\delta\omega_\theta}\right)^2} \\ \qquad \text{for } \omega \in (-\delta\omega_\theta, -\eta\delta\omega_\theta) \text{ or } (\eta\delta\omega_\theta, \delta\omega_\theta), \\ \frac{\eta}{1-\eta} \, \frac{\delta\omega_\theta}{\pi\omega^2} \left[\sqrt{1 - \left(\frac{\omega}{\delta\omega_\theta}\right)^2} - \sqrt{1 - \left(\frac{\omega}{\eta\delta\omega_\theta}\right)^2} \right] \\ \qquad \text{for } \omega \in (-\eta\delta\omega_\theta, \eta\delta\omega_\theta), \\ 0 \qquad \text{otherwise} \,, \end{cases} \tag{9}$$

where $\eta = R_C^2/R^2$ is the volume fraction $0 \le \eta \le 1$. In the limit of small volume fraction the distribution function of the Larmor frequency converges to the Delta function $\delta[\omega]$:

$$\lim_{\eta \to 0} p(\omega) = \delta[\omega] , \tag{10}$$

and in the opposite limit of large volume fractions, i.e., vanishing relaxation volume, the distribution function of the Larmor frequency converges to

$$\lim_{\eta \to 1} p(\omega) = \frac{1}{\pi \delta\omega_\theta \sqrt{1 - \left(\frac{\omega}{\delta\omega_\theta}\right)^2}} . \tag{11}$$

In Fig. 1 the distribution function of the Larmor frequency in the static dephasing limit is shown for different values of the volume fraction. From the magnetic field in Eq. 4 we can see that the minimum value of ω is $-\delta\omega_\theta$ and the maximum value of ω is $+\delta\omega_\theta$. These resonance frequencies are related to spins that are located at the surface of the capillary. Contributions of spins inside the capillary are neglected and therefore higher-resonance frequencies ω are not possible. This means that the distribution function of the Larmor frequency in the static dephasing regime has a compact support. Another important mathematical property is that the distribution function of the Larmor frequency is a purely real function, which is expected from a probability distribution, and furthermore is $p(\omega) = p(-\omega)$, i.e., the distribution function of the Larmor frequency for cylinders is an even function, while the distribution function of the Larmor frequency for spheres [20] has no symmetry relations.

Similar frequency distributions for cylinders are given by Zimmerman and Foster ([26], their Fig. 6). Numerical simulations in terms of a histogram as described above has confirmed the theoretical calculation of $p(\omega)$.

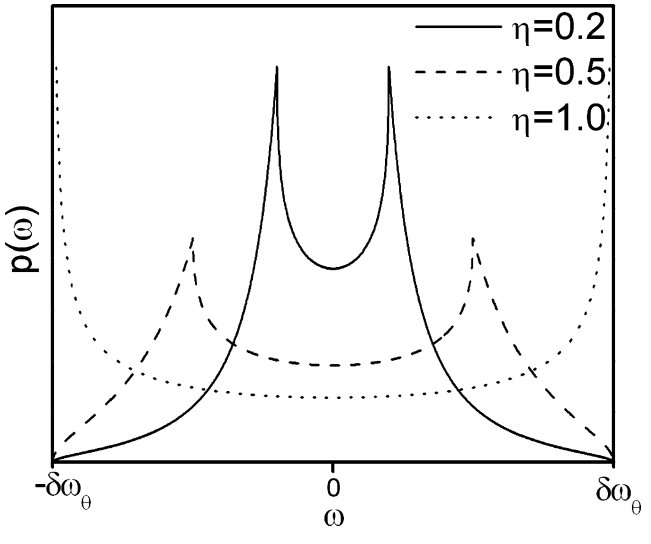

Fig. 1 Distribution function of the Larmor frequency in the static dephasing regime for different volume fraction η. The peaks of the distribution function are located at the frequencies $\omega_{\text{Peak}} = \pm\eta\,\delta\omega_\theta$

The intravascular part represented by the constant internal frequency $\omega_{\text{int}} = 2\delta\omega_{\pi/2}/3 - \delta\omega_\theta$ leads to a Delta peak at the position $\omega = \omega_{\text{int}}$ (see Fig. 5 in [27]).

Of particular interest in MRI is the time course of magnetization decay, which can be obtained from the general expression given in Eq. 1. While the distribution function of the Larmor frequency is only dependent on tissue parameters, the response profile $M_x(\omega) + iM_y(\omega)$ is dependent on the used sequence. In the case of a gradient echo, this transverse magnetization is a constant and we arrive at Eq. 5 for the magnetization decay. Putting the local resonance frequency Eq. 4 in this equation, we obtain an expression for the magnetization decay in the static dephasing regime:

$$M(t) = \frac{M(0)}{1-\eta}\left[g(\eta\,\delta\omega_\theta\, t) - \eta\, g(\delta\omega_\theta\, t)\right] , \tag{12}$$

where the g-function has the property $g(0) = 1$ and is given by

$$g(x) = {}_1F_2\left\{ \begin{matrix} -\frac{1}{2} \\ \frac{1}{2}\ \ 1 \end{matrix} \middle| -\left(\frac{x}{2}\right)^2 \right\} . \tag{13}$$

The generalized hypergeometric function or Barnes extended hypergeometric function is defined as [28]

$${}_pF_q\left\{ \begin{matrix} a_1, \ldots, a_p \\ b_1, \ldots, b_q \end{matrix} \middle| z \right\} = \sum_{k=0}^{\infty} \frac{(a_1)_k \cdot (a_2)_k \cdots (a_p)_k}{(b_1)_k \cdot (b_2)_k \cdots (b_q)_k} \frac{z^k}{k} , \tag{14}$$

and the Pochhammer symbol is given by

$$(x)_k = \frac{\Gamma(x+k)}{\Gamma(x)} . \tag{15}$$

Alternatively, we can reach the same result for the time course of the magnetization decay by introducing the distribution function of the Larmor frequency given in Eq. 9 into the Fourier transform (Eq. 6). According to the mathematical properties of the distribution function of the Larmor frequency, the symmetry $p(\omega) = p(-\omega)$, the reality, and the compact support, the Fourier transform is a purely real function. The result for the magnetization decay given above is in complete agreement with the results of Yablonskiy and Haacke (Eq. 36 in [2]).

In the limit of large volume fraction, where the relaxation volume is converging to an infinitely thin tube, we obtain from Eq. 12 the result

$$\frac{M(t)}{M(0)} = J_0(\delta\omega_\theta\, t) , \tag{16}$$

where J_0 is the Bessel function of the first kind. This result can also be deduced by Fourier transform according to Eq. 6 from the large volume fraction limit of the distribution function of the Larmor frequency given in Eq. 11. According to the general expression for the NMR signal in the static dephasing regime given in Eq. 5, the convergence of the relaxation volume to an infinitely thin tube

leads to a vanishing initial magnetization $M(0)$, while the ratio $M(t)/M(0)$ converges to a Bessel function.

In the short time limit a Taylor expansion of the magnetization decay given in Eq. 12 leads to the expression

$$\frac{M(t)}{M(0)} = 1 - \frac{\eta}{4}\delta\omega_\theta^2 t^2 , \tag{17}$$

i.e., the signal decays quadratically with time, which is in agreement with Eq. 37 given in the paper of Yablonskiy and Haacke [2].

Properties of tissues containing magnetic field inhomogeneities are often characterized by their relaxation time T_2^* or the volume fraction η. The allegation of the relaxation time T_2^* assumes an exponential magnetization decay of the form $M(t) = M(0)\exp(-t/T_2^*)$. Now we are interested in the relaxation time T_2^* that approximates best the exact form of the magnetization decay given in Eq. 12 by a single exponential decay. This relaxation time can be determined according to the *mean relaxation time approximation* [29] as

$$T_2^* = \int_0^\infty \mathrm{d}t \frac{M(t)}{M(0)} . \tag{18}$$

Performing the integration we obtain a simple expression for the transverse relaxation time, and we can find a relation to the distribution function of the Larmor frequency:

$$\begin{aligned} T_2^* &= \frac{1+\eta}{2\eta\delta\omega_\theta} \\ &= \pi p(\omega = 0) , \end{aligned} \tag{19}$$

which can be used to approximate the exact magnetization decay by an exponential function. In Fig. 2 we compare the exact time course of magnetization decay for different values of volume fraction and give the corresponding relaxation time.

Unlike spheres, cylinders can have a tilt angle θ to the external magnetic field (Eq. 3). The distribution function of the Larmor frequency as well as the magnetization decay is dependent on this orientation. An orientation-independent quantity is the marked area in Fig. 3, which is given by

$$A = \frac{2}{\pi}\sqrt{\frac{1+\eta}{1-\eta}} . \tag{20}$$

If the distribution function of the Larmor frequency in the static dephasing limit is given, it is possible to determine the volume fraction η independently of the orientation θ. Once the volume fraction η is found, the equatorial frequency shift $\delta\omega_\theta$ can be found from the peak position itself. Knowing the external magnetic field it is possible to obtain the susceptibility shift and information about the oxygenation state of the blood inside the vessels. For quantification of the volume fraction based on this method, an interval of small resonance frequencies is needed that reflects the signal behavior for long

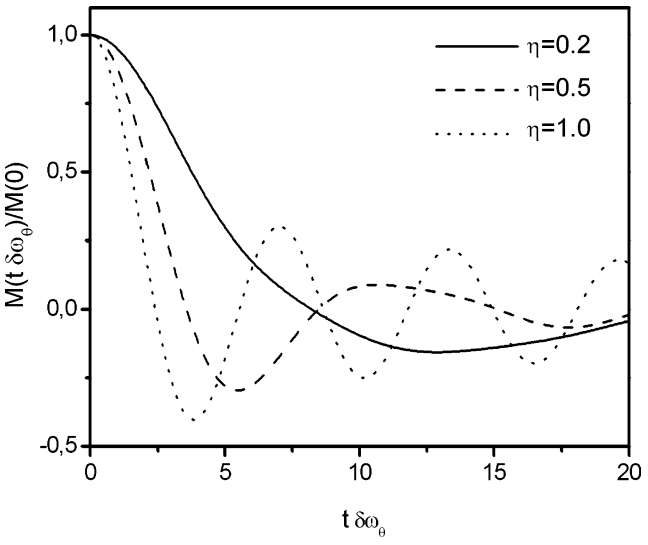

Fig. 2 Magnetization decay for different values of the volume fraction obtained from Eq. 12. If the exact form of the magnetization decay is approximated by a single exponential decay in terms of the *mean relaxation time approximation*, the corresponding relaxation time obtained from Eq. 19 for $\eta = 0.2, 0.5, 1.0$ is $T_2^*\delta\omega_\theta = 3.0, 1.5, 1.0$

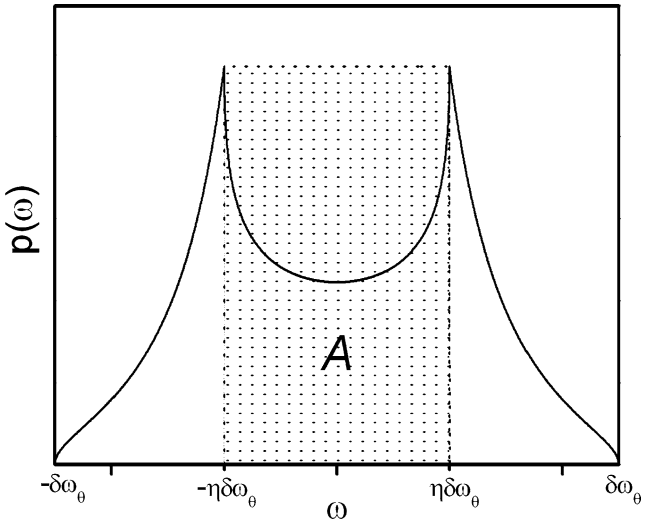

Fig. 3 Determination of volume fraction η. The area of the *marked rectangle A* is given in Eq. 20

durations. However, measurements of the magnetization decay are normally obtained with short echo times, for practical reasons of signal-to-noise.

Discussion

Based on a simple model of a cylindrical voxel containing a vessel, we derived an analytical expression for the distribution function of the Larmor frequency as a function of the volume fraction of blood, the magnetization difference

between vessel and surrounding tissue, and the tilt angle of external magnetic field and vessel axis. The result for the distribution function of the Larmor frequency obtained above is deduced under the assumption that the voxel has a cylindrical shape and its axis coincides with the axis of the vessel. In the case of small volume fractions where the difference between a cylindrical and a cuboid shape of the voxel is negligible, the results can be used for describing the signal received from the voxel. If a system of vessels, for example a vascular network, is considered, the frequency shift due to neighboring capillaries has to be taken into account. In this case the magnetic field in Eq. 2 takes a sum over all capillaries that belong to the network. Since the field from a capillary drops off as $1/r^2$, in the case of small equatorial frequency shifts $\delta\omega_\theta$ the effect of neighboring capillaries can be neglected. Therefore, the distribution function of the Larmor frequency given in Eq. 9 can be used for describing signal formation in a vascular network consisting of a set of parallel cylinders, as for example in the myocardium of the heart. If the voxel is composed of randomly orientated cylinders, an analytical expression for the signal decay is given in Eq. A15 in the paper of Yablonskiy and Haacke [2]:

$$\frac{\underline{M}(t)}{\underline{M}(0)} = \mathrm{e}^{-\eta f(\delta\underline{\omega} t)}, \tag{21}$$

with the function

$$f(x) = \frac{x^2}{20}\left[5\,{}_3F_4\left\{\begin{matrix}\frac{1}{2} & 1 & 1 \\ \frac{5}{4} & \frac{7}{4} & 2\;2\end{matrix}\middle| -\left(\frac{3}{4}x\right)^2\right\} + {}_3F_4\left\{\begin{matrix}1 & 1 & \frac{3}{2} \\ \frac{7}{4} & 2 & 2\;\frac{9}{4}\end{matrix}\middle| -\left(\frac{3}{4}x\right)^2\right\}\right], \tag{22}$$

where the generalized hypergeometric function ${}_3F_4$ is given in Eq. 14. As shown by Yablonskiy and Haacke [2], in the case of randomly distributed cylinders the characteristic frequency is given by the relation

$$\frac{\delta\omega_\theta}{\delta\underline{\omega}} = \frac{3}{2}\sin^2\theta\,. \tag{23}$$

In analogy to the case of a single vessel, we obtain from the backward Fourier transform of Eq. 6 for the distribution function of the Larmor frequency the expression

$$\underline{p}(\omega) = \frac{1}{\pi}\int_0^\infty \mathrm{d}t\,\frac{\underline{M}(t)}{\underline{M}(0)}\cos(\omega t)\,. \tag{24}$$

In Fig. 4 we compare the frequency distribution of a set of parallel cylinders obtained from Eq. 9 with the frequency distribution of a set of randomly distributed cylinders obtained from Eq. 24. In the case of randomly distributed cylinders the distribution function of the Larmor frequency is similar to a Gaussian or Lorentzian one, while in the case of parallel cylinders the distribution function has the characteristic form given in Eq. 9.

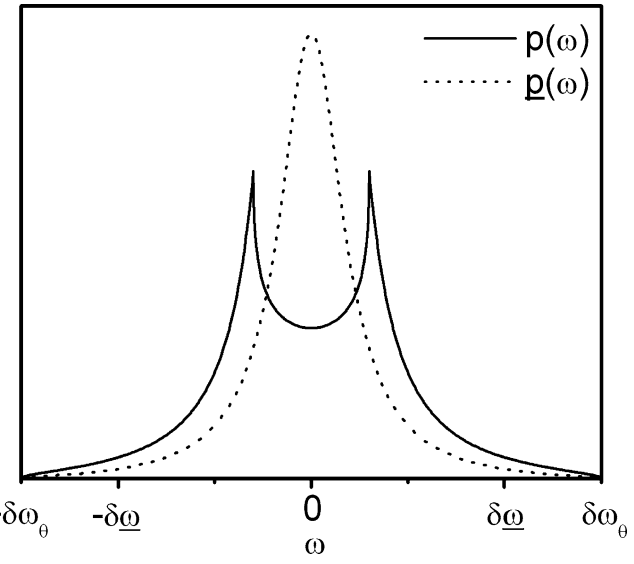

Fig. 4 Comparison of distribution function of Larmor frequency for a set of parallel cylinders $p(\omega)$ and randomly distributed cylinders $\underline{p}(\omega)$ for a volume fraction of $\eta = 0.2$ and a tilt angle of $\theta = 90°$

This distribution function of the Larmor frequency is only dependent on tissue parameters and, therefore, a new characteristic of the vascular network. While former publications only focus on transverse relaxation time obtained from T_2^*-weighted sequences for classification of vascular disease, using this distribution function of the Larmor frequency a general description of NMR-experiments is possible. For example, a TrueFISP experiment can be described by Eq. 1 with the response profile $M_x(\omega) + iM_y(\omega)$ given by Scheffler and Henning [15].

We have focused on the static dephasing regime where diffusion effects can be neglected. Bauer et al. [5–7, 30] developed a rigorous theory to describe diffusion effects and their influence on relaxation time. Diffusion effects will lead to a narrowing of the line shape of the distribution function of the Larmor frequency, which converges to the motional narrowing regime characterized by the transverse relaxation rate $R_2^* = \tau\langle\omega^2(\mathbf{r})\rangle$.

The obtained signal decay shows three types of behavior. For echo times smaller than the relaxation time T_2^*, the signal decays quadratically with time. For intermediate time regimes where the echo time has the same magnitude as the relaxation time, an exponential decay dominates, while for long echo times an oscillating behavior is observed.

Acknowledgements We would like to thank the Schering Stiftung for supporting this work. The authors are indebted to Stephan Glutsch, Walter Nadler, and Nicole Seiberlich for participating in stimulating discussions.

References

1. Kennan RP, Zhong J, Gore JC (1994) Intravascular susceptibility contrast mechanisms in tissues. Magn Reson Med 31:9–21
2. Yablonskiy DA, Haacke EM (1994) Theory of NMR signal behavior in magnetically inhomogeneous tissues: the static dephasing regime. Magn Reson Med 32:749–763
3. Yablonskiy DA, Reinus WR, Stark H, Haacke EM (1997) Quantitation of T2' anisotropic effects on magnetic resonance bone mineral density measurement. Magn Reson Med 37:214–221
4. Yablonskiy DA (1998) Quantitation of intrinsic magnetic susceptibility-related effects in a tissue matrix. Phantom study. Magn Reson Med 39:417–428
5. Bauer WR, Nadler W, Bock M, Schad LR, Wacker C, Hartlep A, Ertl G (1999) Theory of the BOLD effect in the capillary region: an analytical approach for the determination of T2 in the capillary network of myocardium. Magn Reson Med 41:51–62
6. Bauer WR, Nadler W, Bock M, Schad LR, Wacker C, Hartlep A, Ertl G (1999) Theory of coherent and incoherent nuclear spin dephasing in the heart. Phys Rev Lett 83:4215–4218
7. Bauer WR, Nadler W, Bock M, Schad LR, Wacker C, Hartlep A, Ertl G (1999) The relationship between T2* and T2 in myocardium. Magn Reson Med 41:1004–1010
8. Kiselev VG, Posse S (1999) Analytical model of susceptibility-induced MR signal dephasing: effect of diffusion in a microvascular network. Magn Reson Med 41:499–509
9. Kiselev VG, Novikov DS (2002) Transverse NMR relaxation as a probe of mesoscopic structure. Phys Rev Lett 89:278101
10. Kiselev VG (2003) Calculation of diffusion effect for arbitrary pulse sequences. J Magn Reson 164:205–211
11. Jensen JH, Chandra R (2000) NMR relaxation in tissues with weak magnetic inhomogeneities. Magn Reson Med 44:144–156
12. Jensen JH, Chandra R (2000) MR imaging of microvasculature. Magn Reson Med 44:224–230
13. Freeman R, Hill HDW (1971) Phase and intensity anomalies in Fourier transform NMR. J Magn Reson 4:366–383
14. Gyngell ML (1989) The steady-state signals in short-repetition-time sequences. J Magn Reson 81:474–483
15. Scheffler K, Hennig J (2003) Is TrueFISP a gradient-echo or a spin-echo sequence? Magn Reson Med 49(2):395–397
16. Haase A, Frahm J, Matthaei D, Hanicke W, Merboldt K (1986) FLASH imaging: rapid NMR imaging using low flip-angle pulses. J Magn Reson 67:258–266
17. Ogawa S, Lee TM, Kay AR, Tank DW (1990) Brain magnetic resonance imaging with contrast dependent on blood oxygenation. Proc Natl Acad Sci USA 87:9868–9872
18. Mattiello J, Basser PJ, Le Bihan D (1997) The b matrix in diffusion tensor echo planar imaging. Magn Reson Med 37:292–300
19. Reichenbach JR, Haacke EM (2001) High-resolution BOLD venographic imaging: a window into brain function. NMR Biomed 14(7–8):453–467
20. Cheng YC, Haacke EM, Yu YJ (2001) An exact form for the magnetic field density of states for a dipole. Magn Reson Imag 19(7):1017–1023
21. Bakker CJG, Bhagwandien R, Moerland MA, Ramos LMP (1994) Simulation of susceptibility artifacts in 2D and 3D Fourier transform spin-echo and gradient-echo magnetic resonance imaging. Magn Reson Imag 12:767–774
22. Haacke EM, Brown RW, Thompson MR, Venkatesan R (1999) Magnetic resonance imaging: physical principles and sequence design. Wiley, New York
23. Landau LD, Lifshitz EM (1999) Course of theoretical physics, vol 5, 2nd edn. Pergamon, Oxford
24. Durney CH, Bertolina JA, Ailion DC, Christman R, Cutillo AG, Morris AH, Hashemi S (1989) Calculation and interpretation of inhomogeneous line broadening in models of lungs and other heterogeneous structures. J Magn Reson 85:554–570
25. Seppenwoolde JH, van Zijtveld M, Bakker CJ (2005) Spectral characterization of local magnetic field inhomogeneities. Phys Med Biol 50:361–372
26. Zimmerman JR, Foster MR (1957) Standardization of N.M.R. high resolution spectra. J Phys Chem 61:282–289
27. Scheffler K, Seifritz E, Bilecen D, Venkatesan R, Hennig J, Deimling M, Haacke EM (2001) Detection of BOLD changes by means of a frequency-sensitive trueFISP technique: preliminary results. NMR Biomed 14(7-8):490–496
28. Oberhettinger F (1972) Tables of bessel transforms. Springer, Berlin Heidelberg New York
29. Nadler W, Schulten K (1985) Generalized moment expansion for Brownian relaxation processes. J Chem Phys 82:151–160
30. Bauer WR, Nadler W (2002) Spin dephasing in the strong collision approximation. Phys Rev E 65:066123